

REAL-TIME PRECISE DAMAGE CHARACTERIZATION IN SELF-SENSING
MATERIALS VIA NEURAL NETWORK-AIDED ELECTRICAL IMPEDANCE
TOMOGRAPHY: A COMPUTATIONAL STUDY

A Dissertation

Submitted to the Faculty

of

Purdue University

by

Lang Zhao

In Partial Fulfillment of the

Requirements for the Degree

of

Master of Science

May 2020

Purdue University

West Lafayette, Indiana

**THE PURDUE UNIVERSITY GRADUATE SCHOOL
STATEMENT OF DISSERTATION APPROVAL**

Dr. Guang Lin, Chair

School of Mechanical Engineering

Dr. Tyler Tallman

School of Aeronautics and Astronautics

Dr. Liang Pan

School of Mechanical Engineering

Approved by:

Dr. Nicole Key

Head of the School Graduate Program

This is dedicated to my advisors, my friends and my families.

ACKNOWLEDGMENTS

Thanks a lot for the support and help from Professor Lin, Professor Tallman and Professor Pan, without their instruction and profession, this thesis paper cannot be finished. I should also thank the fellows in my research group for their companion and I enjoy the meaningful discussion with them.

During the period of my master program, I have met many great lecturers and kind friends and I have learnt a lot from them, I feel grateful for their help. Finally, I want to thank my parents for their devoted and caring support and love to me, whenever I feel down, they will encourage me and help me regain the courage, their love motivates me to work toward my master's degree.

TABLE OF CONTENTS

	Page
LIST OF TABLES	vii
LIST OF FIGURES	viii
SYMBOLS	ix
ABBREVIATIONS	x
ABSTRACT	xi
1 INTRODUCTION	1
2 ELECTRICAL IMPEDANCE TOMOGRAPHY	4
2.1 EIT forward problem	4
2.2 EIT inverse problem	5
3 DATASET	8
4 METHODOLOGY	10
4.1 Convolutional neural networks	10
4.1.1 Convolutional layer	10
4.1.2 Pooling layer	11
4.1.3 Fully connected layer	12
4.1.4 Softmax	12
4.2 K-means	12
5 CASE STUDIES	14
5.1 Predict the number of holes	14
5.1.1 Problem Setting	14
5.1.2 Using EIT Images	14
5.1.3 Using Conductivity Change Vectors	16
5.2 Predict the radius of holes	20
5.2.1 Problem Setting	20

	Page
5.2.2 Using EIT Images	20
5.2.3 Using Conductivity Change Vectors	22
5.3 Predict the center position of holes	24
5.3.1 Problem Setting	24
5.3.2 Using EIT Images	25
5.3.3 Using Conductivity Change Vectors	26
5.4 Conclusion	27
6 SUMMARY	30
REFERENCES	31

LIST OF TABLES

Table	Page
5.1 The detailed specifications of CNN predicting the number of holes	16
5.2 The detailed specifications of FCNN predicting the number of holes	18
5.3 The detailed specifications of CNN predicting the radius of holes	21
5.4 The detailed specifications of FCNN predicting the radius of holes	23
5.5 The detailed specifications of FCNN predicting the center positions of holes	27
5.6 Comparison of performance between using EIT images and conductivity change vectors as input	28

LIST OF FIGURES

Figure	Page
1.1 An example of EIT generated image [2]	3
2.1 Sample EIT image with colorbar presenting conductivity change distribution	7
3.1 Conductivity change distribution vector and corresponding finite element mesh	9
3.2 An EIT image in the form of matrix	9
4.1 Kernel in the Convolutional Layer [7]	11
4.2 Max Pooling Layer	11
4.3 Steps of K-means [9]	13
5.1 Preprocessing process for EIT images	15
5.2 The structure of the Convolutional Neural Network predicting the number of holes	16
5.3 Training process of the CNN predicting the number of holes	17
5.4 The structure of Fully Connected Neural Network predicting the number of holes	18
5.5 Training process of the FCNN predicting the number of holes	19
5.6 Structure of the CNN predicting the radius of Holes	21
5.7 Training process of the CNN predicting the radius of holes	22
5.8 The structure of Fully Connected Neural Network predicting the hole radius	23
5.9 Training process of the FCNN predicting the radius of holes	24
5.10 The structure of Fully Connected Neural Network predicting the center position of holes	26
5.11 Training process of the FCNN predicting the center position of holes	28
5.12 Comparison of performance between using EIT images and conductivity change vectors as input	29

SYMBOLS

σ	conductivity distribution
ϕ	domain potential
z_l	contact impedance at the l th electrode
V_l	voltage on the l th electrode
A_M	usual stiffness matrix for steady-state diffusion
Φ	vector of the nodal voltages
V	vector of electrode solutions
I	vector of currents applied to electrodes
φ_i	i th finite element interpolation function
δV	difference between the two sets of voltage data measured at two time point
$F(\cdot)$	operator that calculate the voltage form conductivity
σ_0	background conductivity
$\delta\sigma$	conductivity change that the inverse process seeks to predict
J	sensitivity matrix

ABBREVIATIONS

SHM	structural health monitoring
EIT	electrical impedance tomography
CNN	convolutional neural networks
FCNN	fully connected neural network
MSE	mean squared error
ReLU	rectified linear unit

ABSTRACT

Lang, Zhao M.S., Purdue University, May 2020. Real-Time Precise Damage Characterization in Self-Sensing Materials via Neural Network-Aided Electrical Impedance Tomography: A Computational Study. Major Professor: Guang Lin.

Many cases have evinced the importance of having structural health monitoring (SHM) strategies that can allow the detection of the structural health of infrastructures or buildings, in order to prevent the potential economic or human losses. Nanocomposite material like the Carbon nanofiller-modified composites have great potential for SHM because these materials are piezoresistive. So, it is possible to determine the damage status of the material by studying the conductivity change distribution, and this is essential for detecting the damage on the position that cannot be observed by eye, for example, the inner layer in the aerofoil. By now, many researchers have studied how damage influences the conductivity of nanocomposite material and the electrical impedance tomography (EIT) method has been applied widely to detect the damage-induced conductivity changes. However, only knowing how to calculate the conductivity change from damage is not enough to SHM, it is more valuable to SHM to know how to determine the mechanical damage that results in the observed conductivity changes. In this article, we apply the machine learning methods to determine the damage status, more specifically, the number, radius and the center position of broken holes on the material specimens by studying the conductivity change data generated by the EIT method. Our results demonstrate that the machine learning methods can accurately and efficiently detect the damage on material specimens by analysing the conductivity change data, this conclusion is important to the field of the SHM and will speed up the damage detection process for industries like the aviation industry and mechanical engineering.

1. INTRODUCTION

The process of implementing a damage identification strategy for aerospace, civil and mechanical engineering infrastructure is referred to as structural health monitoring (SHM) [1]. SHM provides cost-effective and reliable inspection and monitoring solutions to ensure safety and reliability of structures, so it can help improve reliability of existing infrastructure and design structures with a much longer service life. Nanocomposite material like the Carbon nanofiller-modified composites attracts much attention from researchers studying SHM since the nanocomposite material is piezoresistive and therefore self-sensing. This means the conductivity of the nanocomposite material is tightly relevant to the stress and damage on the material, this material shows a detectable change in their electrical conductivity with applied strain or damage.

Because of the characteristic of the self-sensing material, the method that is capable of measuring the conductivity distribution through the material is highly required. The electrical impedance tomography (EIT) is a good approach to estimate the electrical conductivity distribution of material and it has been used widely since this method can continuously and non-invasively generate vectors and images to represent the conductivity distribution through the material, and from the conductivity distribution, the mechanical state can be deduced. With these advantages, EIT has been used widely for the strain and damage detection. For example, Loh et al [2]. comes up with a new carbon nanotube-polyelectrolyte sensing skin, this skin is fabricated via the layer-by-layer technique, since this skin is self-sensing, it can be used to detect the damage and stress on the skin, the layer-by-layer approach is based on the sequential adsorption of oppositely charged polyelectrolyte and nanomaterial species to form homogeneous percolated nanostructures. In their study, EIT is applied on the newly proposed material to offer the two-dimensional damage maps, in

the experiment, 32 copper tape electrodes are set around the boundary of material for the implement of EIT. A pendulum impact testing apparatus is constructed in the experiment as the damage to be detected, and on each specimen, four impacts are induced. Finally, EIT is applied to detect damage, on the generated map, the existence of damage can be found and people can have a general idea where the damage is as shown in Fig.1.1.. The application of using EIT for damage characterization is extended by the research of Dai and Gallo et al. [3]. In their study, the sensor consists of a nonwoven aramid fabric is used, which is first coated with nanotubes using a solution casting approach and then infused with epoxy resin through the vacuum assisted resin transfer molding technique. They also improve the EIT by employing a newly defined adjacent current–voltage measurement scheme associated with 32 electrodes applied along the periphery of the sensor, with the improvement, their method can generate EIT maps for more categories of damage including square holes, crack and progressive impacts.

References introduced above have already shown that EIT can be used to detect the damage on self-sensing material and the potential of EIT for SHM, however, since the result of these studies is the EIT image that is in low resolution as shown in Fig.1.1., we can only determine the existence of damage and have a general idea of where the damage is, but the detailed information of damage status like the number, exact location and severity of damage cannot be determined by applying their method, and this information is essential to SHM since it is an important evidence for the evaluation of the health status of structure, therefore, it is necessary to go a step further to come up with a new method that can understand the output data of EIT and determine the detailed information of the damage status like the number, location and severity of damage.

In this study, We intend to combine machine learning algorithms especially the neural network and EIT to determine the damage status on the self-sensing material specimens, since neural network is very capable of identifying the nonlinear relationship between input and the output.

In our study, we use a EIT simulation program to generate the conductivity change distribution vectors and images constructed from the vectors as the dataset, both categories of data represent the conductivity change distribution through a specimen. All damage on the specimens used in simulation is circular. We apply machine learning methods like the fully connected neural network and convolutional neural network on the EIT generated data to determine the damage status, and compare the performance of models using vectors and images as input separately.

Compared to the traditional ways of using EIT for damage detection, our method not only finds the existence of damage but also give a much more precise description of the damage status, and after our model is well trained, it can achieve the real-time and accurate damage detection for new samples which shows a great potential to the field of SHM.

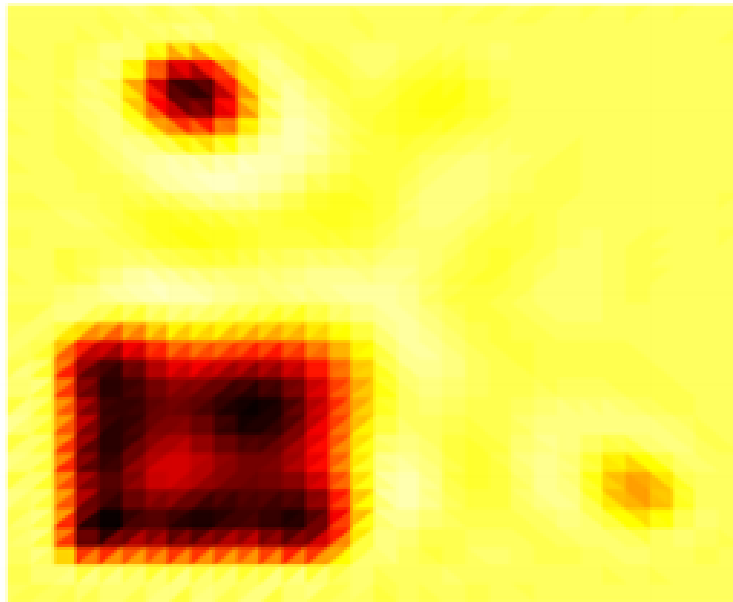


Fig. 1.1. An example of EIT generated image [2]

2. ELECTRICAL IMPEDANCE TOMOGRAPHY

2.1 EIT forward problem

EIT is a soft-field tomography technique that aims to determine the conductivity distribution of a detected domain using electrical excitations and corresponding voltage measurements obtained along the domain's periphery [4]. To apply the EIT method, electrodes are located to the periphery of the domain being examined. Small alternating currents will be injected between a pair of neighboring electrodes, and the resulting voltage is measured between electrode pairs not involved in the current injection [5]. The injection of current will be applied to the next pair of electrode and this action will be repeated until every pair of electrode has been applied a injection of current. Flow of electric charge through the conductive domain is governed by Laplace's equation that is shown in equation (2.1) where the electric potential distribution is ϕ and the conductivity distribution is σ .

$$\nabla \cdot \sigma \nabla \phi = 0 \quad (2.1)$$

Contact impedance between the electrodes and the examined domain is shown in equation (2.2), which is used to calculate the boundary electrode voltages. Equation (2.3) shows the conservation of charge. In equations (2.2) and (2.3), n is a normal vector pointing outward, z_l is the contact impedance at the l th electrode and V_l is the measured voltage at the l th electrode, and N is the total number of electrodes.

$$z_l \sigma \nabla \phi \cdot \mathbf{n} = V_l - \phi \quad (2.2)$$

$$\sum_{l=1}^N \int_{E_l} \sigma \nabla \phi \cdot \mathbf{n} dS_l = 0 \quad (2.3)$$

The finite element approach can be used to solve the problem as shown in equation (2.4),

$$\begin{bmatrix} A_M + A_Z & A_W \\ A_W^T & A_D \end{bmatrix} \begin{bmatrix} \Phi \\ V \end{bmatrix} = \begin{bmatrix} 0 \\ I \end{bmatrix} \quad (2.4)$$

$$A_{Zij} = \sum_{l=1}^N \int_{E_l} \frac{1}{z_l} \varphi_i \varphi_j dS_l \quad (2.5)$$

$$A_{Wli} = - \int_{E_l} \frac{1}{z_l} \varphi_i dS_l \quad (2.6)$$

$$A_D = \text{diag} \left(\frac{E_l}{z_l} \right) \quad (2.7)$$

Here, A_M is the usual stiffness matrix for the governing equation to the numerally meshed 2-D domain, Φ is a vector of the nodal voltages, V is a vector of electrode solutions, I is a vector of current injections applied to the electrodes, and φ_i is the interpolation function for the i th finite element. Equation (2.4) is only solved up to an additive constant (i.e. a ground point). However, because EIT makes use of the difference between electrode voltages, this is inconsequential.

2.2 EIT inverse problem

While in the EIT forward problem, the conductivity distribution of the examined domain is known and the boundary voltage data is predicted from the conductivity distribution, the inverse problem predicts the conductivity distribution from the measured boundary voltage data. The EIT inverse problem is nonlinear, so a one-step linearization is used to estimate the electrical conductivity change between two measurements in time. That is, one vector of voltage is measured from the domain before deformation and a second vector of voltage is measured after deformation, EIT will predict the conductivity change that causes the difference between the two sets of measured voltage data.

$$\delta V = V(\sigma_2, t_2) - V(\sigma_1, t_1) \quad (2.8)$$

$$W(\delta\sigma) = F(\sigma_0 + \delta\sigma) - F(\sigma_0) \quad (2.9)$$

In the equation (2.8), δV is the difference between the two sets of voltage data measured at time t_1 and t_2 . $F(\cdot)$ is the operator that calculates the voltage from conductivity, σ_0 is the background conductivity and $\delta\sigma$ is the conductivity change that the inverse process seeks to predict. To solve the inverse problem, the vector $\delta\sigma$ that minimizes the difference between δV and $W(\delta\sigma)$ needs to be found. The forward operator can be linearized as $F(\sigma_0 + \delta\sigma) \approx F(\sigma_0) + J\delta\sigma$, J is the sensitivity matrix and $J = \partial F(\sigma_0) / \partial\sigma$, with equation (2.9), the conductivity change distribution that results in the minimization of the voltage difference can be written as equation (2.10). The last term in equation (2.10) is a regularization term.

$$\delta\sigma^* = \arg \min_{\delta\sigma \geq 0} \|J\delta\sigma - \delta V\|^2 + \kappa \|L\delta\sigma\|^2 \quad (2.10)$$

The Fig.2.1. is an example of the image constructed from the conductivity change distribution predicted by EIT, since the damage domain loses the electrical conductivity, its color is different from the color of the background. The pixel value vector of a patch of domain reflects its conductivity change value, which is shown clearly in the Fig.2.1..

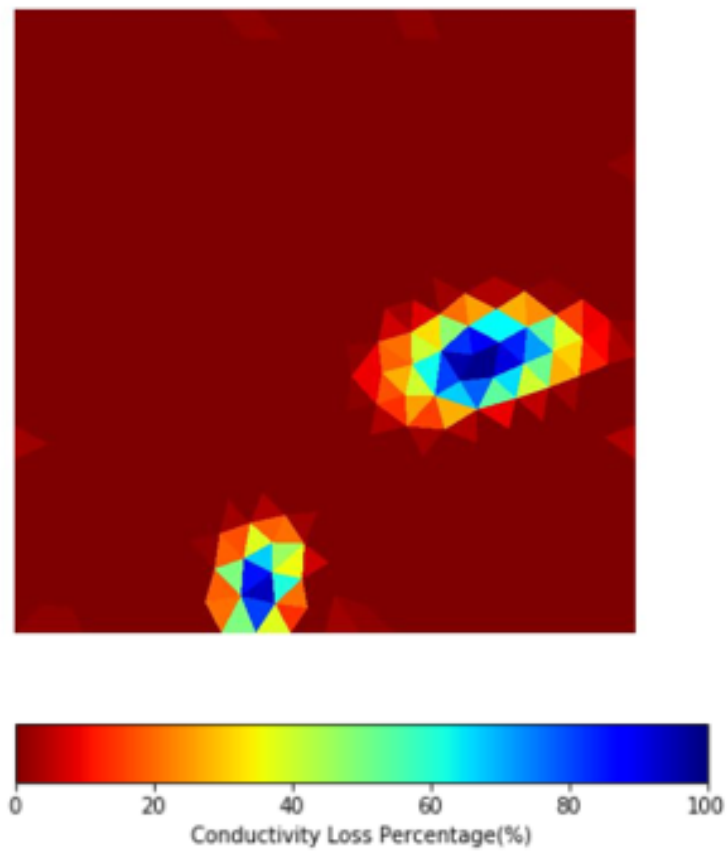


Fig. 2.1. Sample EIT image with colorbar presenting conductivity change distribution

3. DATASET

A large amount of data is required in our study, and all data used in our study is generated by a EIT simulation program. The specimen used in the simulation is in the size of 0.9m by 0.9m. All damage studied in our study is circular and each specimen has at least 1 circular damage, at most 3 circular damage. For the balance of data, one third of generated samples have 1 hole, one third have 2 holes and one third have 3 holes. Each circular damage is in the radius between 0.03 to 0.05m. The finite element mesh for the EIT reconstruction has 772 triangular cells.

As mentioned in the last chapter, EIT generates two categories of data, conductivity change distribution vectors and images constructed from the vectors. For the vector, its length is 772 which equals to the number of cells in the EIT finite element mesh and each element in the vector represents the conductivity change value of the corresponding cell which is shown in Fig.3.1.. For the images, they are stored as 538-by-538-by-3 data matrix that shows the red, green, and blue color components for each individual pixel which is shown in Fig.3.2., the width and height of the image is 538 pixels. Both categories of data represent the conductivity change distribution through a specimen and in this study, both of them are considered as input of models trained in this study.

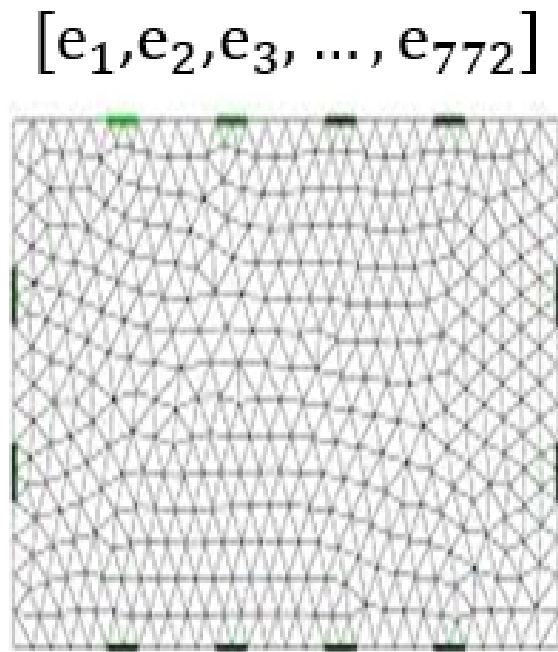


Fig. 3.1. Conductivity change distribution vector and corresponding finite element mesh

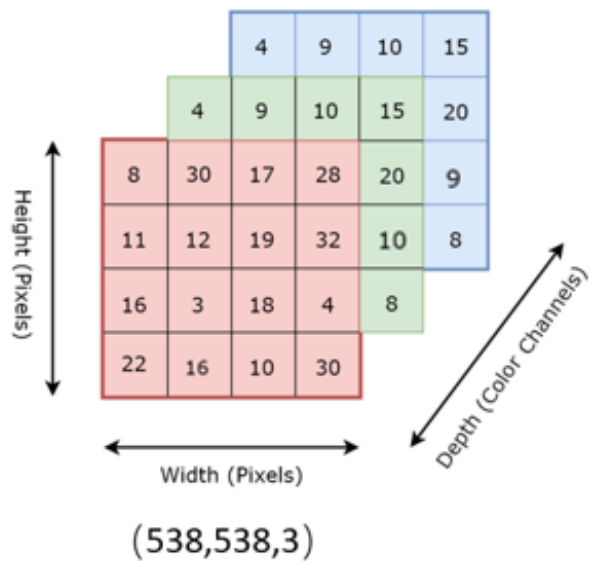


Fig. 3.2. An EIT image in the form of matrix

4. METHODOLOGY

The goal of our study is to detect the damage status on self-sensing material specimen by analyzing the EIT generated conductivity change distribution data with machine learning methods. This goal can be divided into predicting the number, the radius and the center position of the damage holes. For EIT images, we use Convolutional Neural Networks(CNN) to predict the number and radius of holes and use K-means to predict the center position of holes. For conductivity change vectors, we use fully connected neural networks(FCNN) to detect the damage status.

4.1 Convolutional neural networks

Convolutional neural network is one of the variants of neural networks which is frequently applied to analyzing images. In this section, the most important theories and concepts of convolutional neural network are described.

4.1.1 Convolutional layer

A Convolutional Layer is essential in CNNs since it is used to detect features and has several kernels with learnable weights [6]. Kernels work as filters and a kernel is a matrix of integers as is shown in Fig.4.1.. Each kernel provides a measure for how close a patch of input resembles a feature, a kernel slides over the complete image and dot product is taken between the kernel and a patch of image, the greater the result, the closer the patch of image resembles the feature. The computed dot product values corresponding to the channels of each kernel are summed up with a bias to produce the results of each kernel. These results form the spatial feature maps of the convolutional layer.

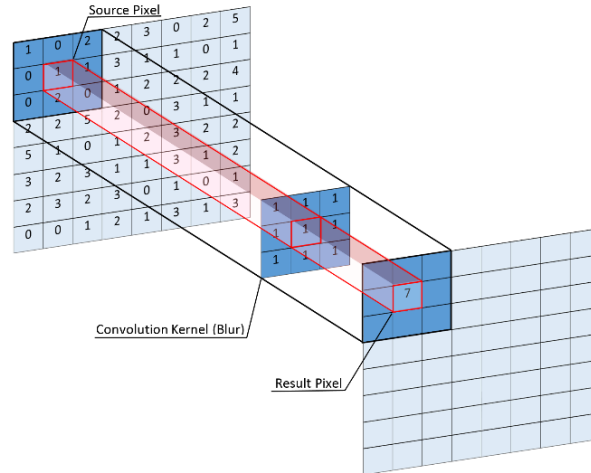


Fig. 4.1. Kernel in the Convolutional Layer [7]

4.1.2 Pooling layer

The next stage is the pooling layer, where the features extracted by the convolutional layer are selected for downsampling, which reduces computational cost. The function of the pooling layer is straightforward; for example, max pooling layer extracts the maximum in the feature maps after convolutional layer; average pooling layer extracts the averages in the feature maps after convolutional layer [8].

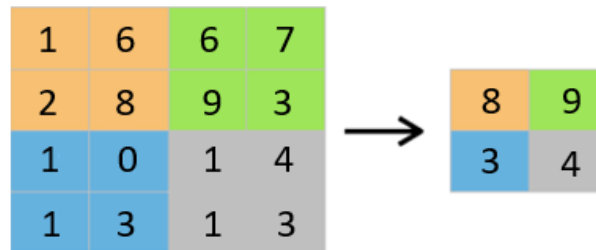


Fig. 4.2. Max Pooling Layer

4.1.3 Fully connected layer

Fully connected layer is an essential component of convolutional neural networks and it connects to all neurons in the previous layer. It takes the outputs of the previous layer, performs dot product between the weights of each neuron and the input and adds a bias in each neuron.

4.1.4 Softmax

The softmax function is an activation function usually used in the classification model to predict the class of the input. The softmax function takes the output from the previous fully connected layer, estimates the probabilities for each class, and predicts the class that has the greatest probability as the prediction of the classification model

4.2 K-means

K-means algorithm is an clustering algorithm that is capable of partitioning the dataset into K distinct clusters, and these clusters should not overlap each other, each data point in the dataset belongs to only one cluster. K-means tries to make the data points inside a cluster as close as possible while keeping the data points in different clusters as far as possible. It randomly select K data points as initial centroids then the sum of the squared distance between data points and all centroids is calculated, each data point is assigned to the closest centroid, then centroids for the clusters are calculated by taking the average of the all data points that belong to each cluster, these steps are iterated until the centroids cannot be changed any more.

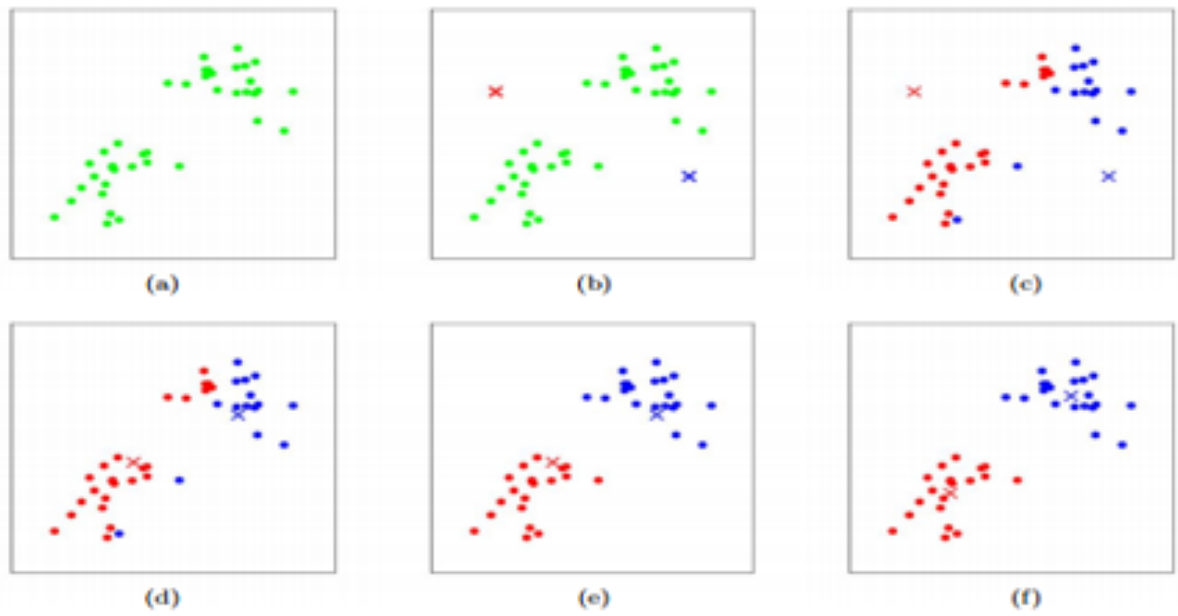


Fig. 4.3. Steps of K-means [9]

5. CASE STUDIES

5.1 Predict the number of holes

5.1.1 Problem Setting

In this section, the principal idea is to create a model that can predict the number of holes given the EIT generated conductivity change data. Since the number of holes on a material specimen is between 1 to 3, the problem of predicting the number of holes can be seen as a multiclass classification problem, the class 1, class 2 and class 3 represents that this specimen has 1, 2 and 3 holes.

5.1.2 Using EIT Images

A convolutional neural network is applied to predict the number of hole with EIT images.

Data Preprocessing

Noise is observed on EIT images which influences the performance of our model, in order to avoid this, the red color component for each individual pixel is removed. In order to reduce the dimension of input and accelerate the model training process, the input images are resized to 100 * 100-pixel by applying interpolation. Pixel values of images are normalized to 0 to 1 by dividing all pixel values by 255 which will improve the performance of the model and speed up the training process, the preprocessing steps are shown in Fig.5.1..

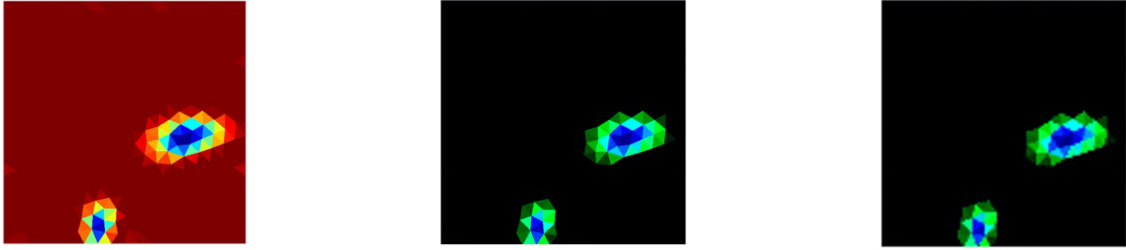


Fig. 5.1. Preprocessing process for EIT images

Convolutional Neural Network Structure

In the convolutional neural network used to predict the number of holes, the first layer is the convolution layer that has 16 kernels and the size of each kernel is 3 by 3, the second layer is a Batch Normalization layer added to improve accuracy and speed up training by solving the internal covariate shift problem of the previous layer, the third layer is a Max Pooling layer used to reduce the complexity of computation by reducing the dimensionality of the input, the fourth layer is a Flatten layer that flattens the input to 1-dimensional array, the fifth layer is a Dense layer that has 256 nodes to capture all the information contained in the input of this layer, the sixth layer is a Dropout layer used to prevent overfitting and the output layer is a Dense layer that has three nodes and the activation function is softmax since the model works as a classifier. The Fig.5.2. and the Table 5.1. present the details of structure of the convolutional neural network clearly.

Experiment and Result

In this section, an experiment is conducted using the previously proposed convolutional neural network. The network is trained and tested using EIT images.

7650 EIT images are used to train and validate the convolutional neural network, in the training process, 1500 epochs and batch size 32 have been used when feeding in the training samples, after the training, the model's performance on 1350 testing

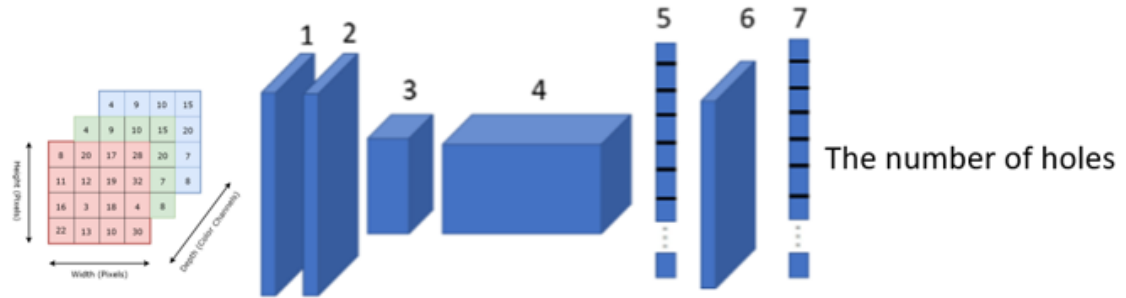


Fig. 5.2. The structure of the Convolutional Neural Network predicting the number of holes

Table 5.1.

The detailed specifications of CNN predicting the number of holes

Layer	Type	Depth	Kernel Size	Stride
1	CONV+ReLU	16	3*3	1
2	BatchNormalization	-	-	-
3	Max pooling	-	-	-
4	Flatten	-	-	-
5	FC	256	-	-
6	Dropout	-	-	-
7	FC+Softmax	3	-	-

images gives the accuracy of 0.892. Fig.5.3. shows the training accuracy and the validation accuracy plots against epochs.

5.1.3 Using Conductivity Change Vectors

A fully connected neural network is used to predict the number of holes with the conductivity change vectors as a classification model.

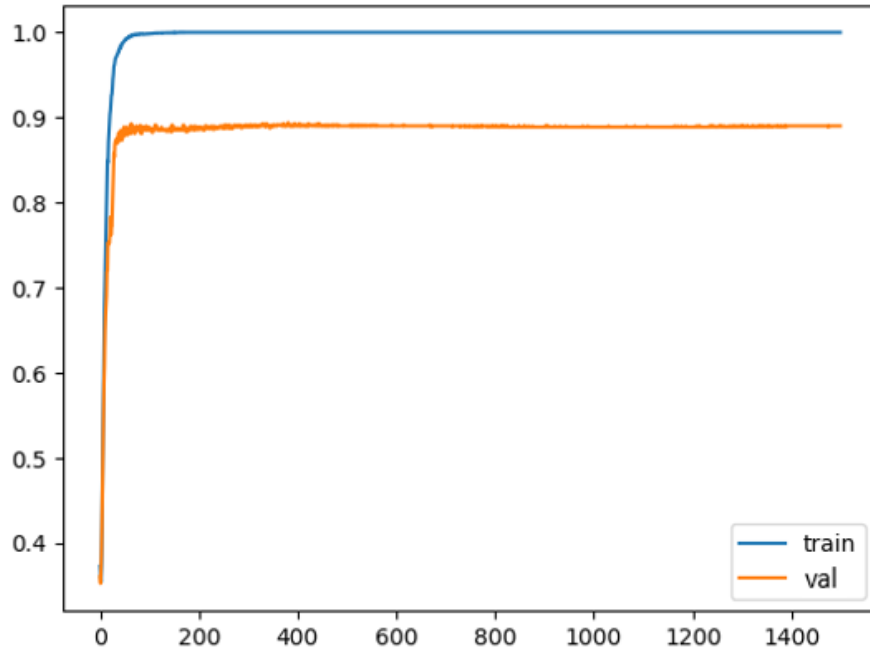


Fig. 5.3. Training process of the CNN predicting the number of holes

Data Preprocessing

The conductivity change vector is normalized to a unit vector by dividing every element by the norm of the vector which can speed up the gradient descent process and improve the performance and stability of our model.

Fully Connected Neural Network Structure

We choose to use a fully connected neural network to predict the number of holes with the conductivity change vectors as a classification model. The proposed network is composed of 1 input layer, 3 hidden layers and 1 output layer. The input layer contains 772 neurons, each of them represents an element in the conductivity change vector. The number of neurons in the first hidden layer is 256, which is enough to understand all the information contained in the input layer. There are 64 and 16 neurons in the next two hidden layers. The activation function called ReLU is

applied in neurons in hidden layers. In the output layer, there are three neurons and the activation function is softmax function since our model is a three-classes classifier. The Fig.5.4. and the Table 5.2. present the structure of the fully connected neural network more clearly.

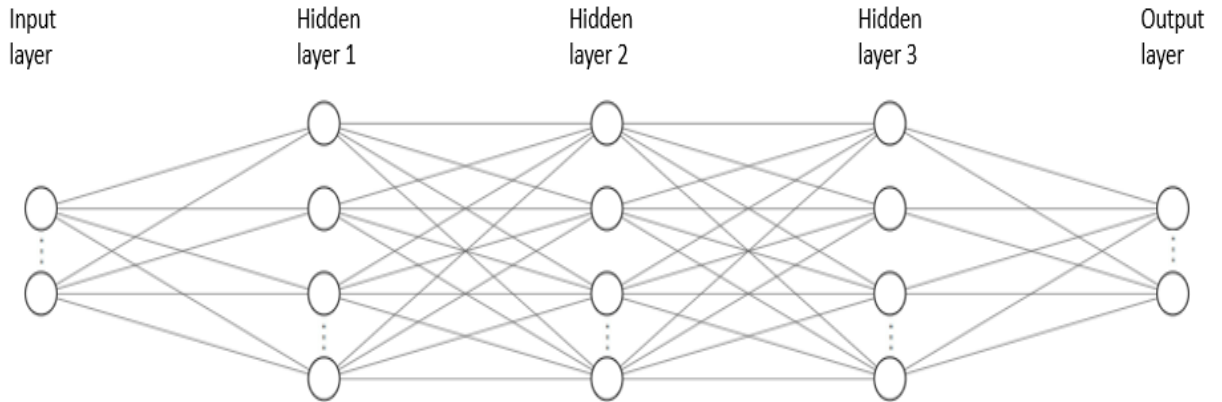


Fig. 5.4. The structure of Fully Connected Neural Network predicting the number of holes

Table 5.2.

The detailed specifications of FCNN predicting the number of holes

Layer	Type	Units
1	FC+ReLU	256
2	FC+ReLU	64
3	FC+ReLU	16
4	FC+Softmax	3

Experiment and Result

In this section, an experiment is conducted using the previously proposed fully connected neural network. 16800 conductivity change vectors are used to train and validate the fully connected neural network, 700 epochs and batch size 32 have been applied in the training process, after the training, the model's performance on 4200 testing samples gives the accuracy of 0.995. Fig.5.5. shows the training accuracy and the validation accuracy plots against epochs. From the result, we can see the improvement of accuracy compared to the result of using EIT images as input.

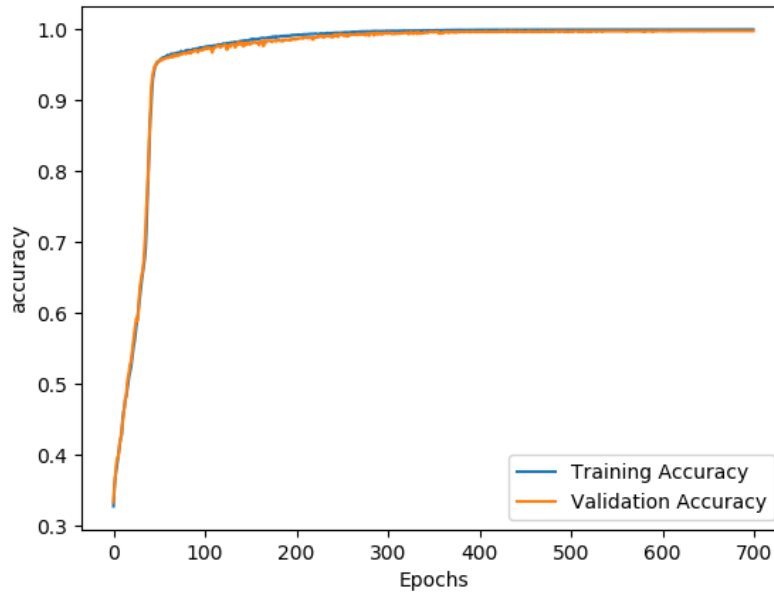


Fig. 5.5. Training process of the FCNN predicting the number of holes

5.2 Predict the radius of holes

5.2.1 Problem Setting

In order to detect the degree of damage on the material specimens, we need to detect the radius of damage holes. In this section, we create a generic model that can predict the radius of holes on material specimens given the EIT generated conductivity change data. Since the distribution of radius is continuous, this task can be seen as a regression problem. With the EIT images as input, we train a convolutional neural network to predict the radius of holes, with the conductivity change vectors as input, a fully connected neural network is used as a regression model.

5.2.2 Using EIT Images

Dataset and Data Preprocessing

The dataset we use in this section is same as the EIT images used in predicting the number of holes and the images are prepossessed in the same way.

Convolutional Neural Network Structure

The structure of the CNN predicting the radius of holes is similar to that predicting the number of holes, the only difference is that the output layer has no activation function since the convolutional neural network is a regression model. The Fig.5.6. and the Table 5.3. present the structure of the CNN clearly.

Experiment and Result

In this section, an experiment is conducted using the previously proposed convolutional neural network. 7650 EIT images are used to train and validate the neural network, after the training, the model is tested on 1350 images and the performance

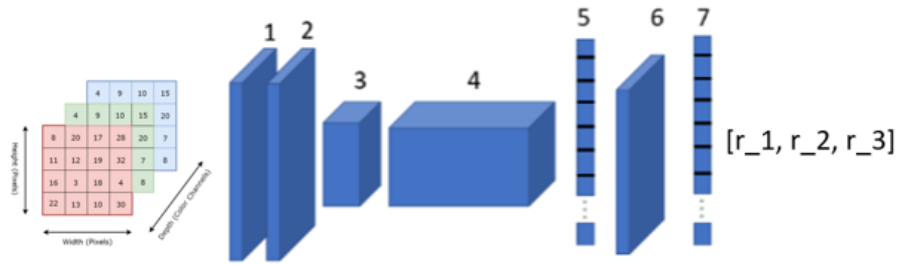


Fig. 5.6. Structure of the CNN predicting the radius of Holes

Table 5.3.

The detailed specifications of CNN predicting the radius of holes

Layer	Type	Depth	Kernel Size	Stride
1	CONV+ReLU	16	3*3	1
2	BatchNormalization	-	-	-
3	Max pooling	-	-	-
4	Flatten	-	-	-
5	FC+ReLU	256	-	-
6	Dropout	-	-	-
7	FC	3	-	-

using MSE gives the testing error of 1.01×10^{-4} , by comparing the predicted output and the annotation, the average difference between the predicted and true radius is 0.00765m. Fig.5.7. shows the training process.

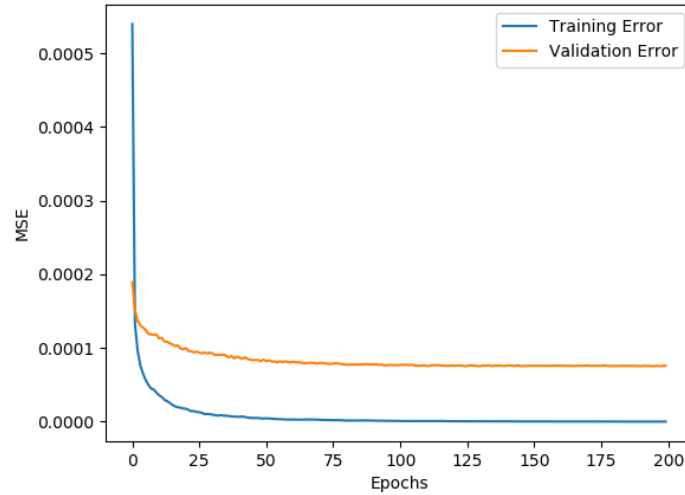


Fig. 5.7. Training process of the CNN predicting the radius of holes

5.2.3 Using Conductivity Change Vectors

Dataset and Data Preprocessing

The dataset we use in this problem is same as the conductivity change vectors used in predicting the number of holes and we preprocess the vectors in the same way.

Fully Connected Neural Network

The structure of the fully connected neural network predicting the radius is almost the same as that predicting the number of holes except that no activation function is applied on the output layer in this network since the model is a regression model. The Fig.5.8. and the Table 5.4. present the structure of the fully connected neural network clearly.

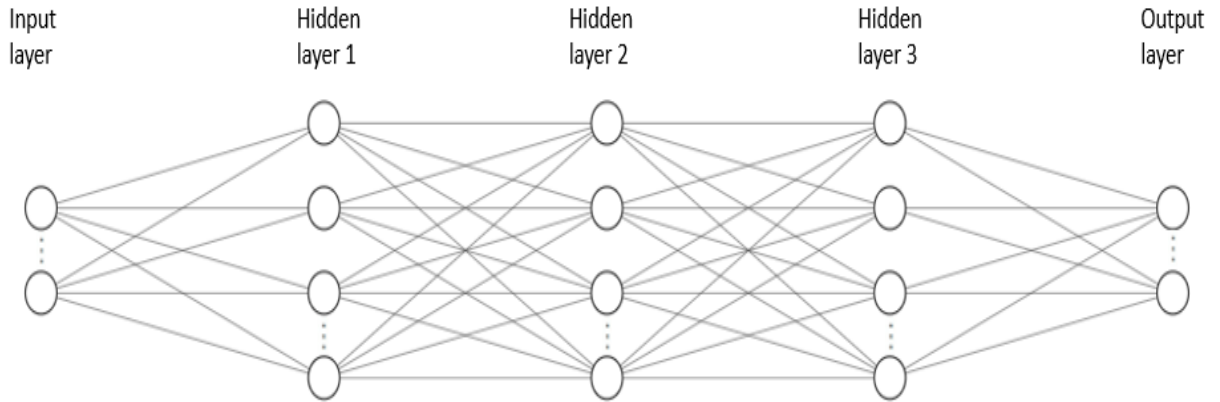


Fig. 5.8. The structure of Fully Connected Neural Network predicting the hole radius

Table 5.4.
The detailed specifications of FCNN predicting the radius of holes

Layer	Type	Units
1	FC+ReLU	256
2	FC+ReLU	64
3	FC+ReLU	16
4	FC	3

Experiment and Result

In this section, an experiment is conducted using the previously proposed fully connected neural network. 16800 conductivity change vectors are used to train and validate the fully connected neural network, after the training, the model's performance on 4200 testing samples using MSE gives the testing error of 4.85×10^{-6} , by comparing the predicted output and the annotation, the average difference between the predicted and true radius is 0.000872m. Fig.5.9. shows the training process.

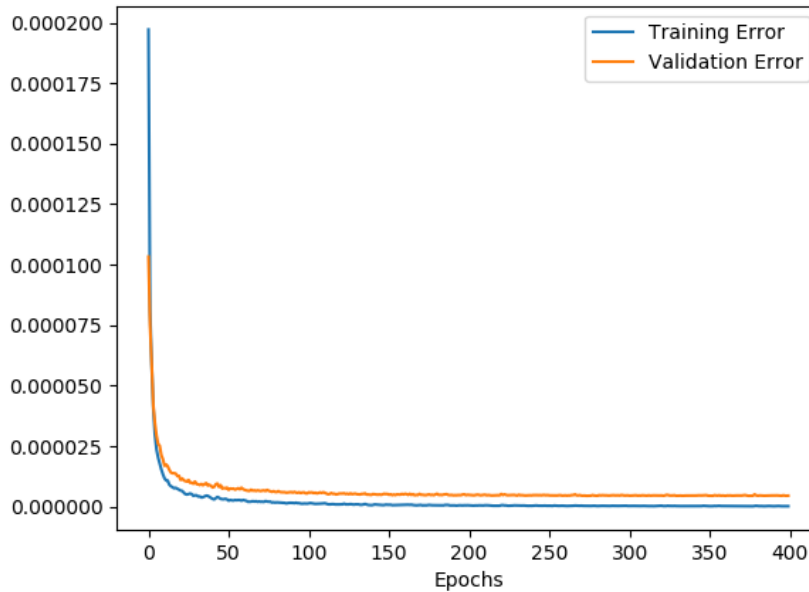


Fig. 5.9. Training process of the FCNN predicting the radius of holes

5.3 Predict the center position of holes

5.3.1 Problem Setting

In order to localize the damage, we need to predict the center position of holes. On the EIT images, a damage hole can be seen as a cluster of pixels, therefore, the clustering algorithms can be applied to predict the center position of holes. Unlike the neural networks we introduced above, the clustering algorithms are unsupervised machine learning algorithms, so we do not need to provide annotation of samples to the algorithm. In our study, the K-means algorithm is used and the coordinates of the pixels that form the damage domain on the image are fed to the K-means, K-means divides the coordinates into K clusters, K is the number of damage holes, and K-means can also output the centroids for the K clusters, we can approximately see the K centroids as the centers of holes.

With using the conductivity change vectors as input, this problem can be treated as a regression problem, so we apply a fully connected neural network as a regression model to predict the center position of holes with the vectors as a regression model.

5.3.2 Using EIT Images

Dataset and Data Preprocessing

The dataset we use in this section is same as the EIT images used in predicting the number and radius of holes and we remove the red color component for each individual pixel to remove the noise and background on the image, only the pixels that form the damage domain are reserved.

K-means Clustering

The first step of using the K-means algorithm is specifying the number of clusters K , which is the number of holes on the image in our study, since our model of predicting the number of holes has a good accuracy, we can assume that we have already known the value of K . After we preprocess the EIT images, only the pixels that form the damage domain are reserved, and we can find the coordinates of these pixels. We use the K-means algorithm with the coordinates, and K-means will predict the center position for the K holes.

Experiment and Result

After the model is fed with 9000 samples, by comparing the predicted output and annotations, the average distance between predicted and true center position is 0.0172m.

5.3.3 Using Conductivity Change Vectors

Dataset and Data Preprocessing

The dataset we use in this problem is same as the conductivity change vectors used in predicting the number and radius of holes and we preprocess the images in the same way.

Fully Connected Neural Network Structure

The structure of the fully connected neural network used here is similar to that used in predicting the radius, except we add a dense layer with 32 neurons after the second dense layer to improve the ability of model to represent more complicated functions and the output layer has six nodes since for each hole, we need to predict the x-coordinate and y-coordinate of its center. The Fig.5.10. and the Table 5.5. present the structure of the fully connected neural network more clearly.

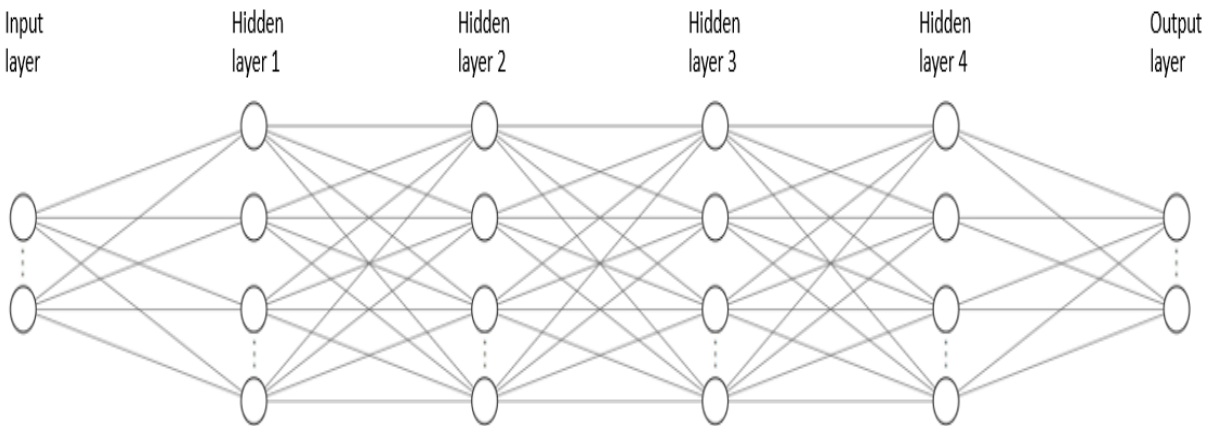


Fig. 5.10. The structure of Fully Connected Neural Network predicting the center position of holes

Table 5.5.
The detailed specifications of FCNN predicting the center positions of holes

Layer	Type	Units
1	FC+ReLU	256
2	FC+ReLU	64
3	FC+ReLU	32
4	FC+ReLU	16
5	FC	6

Experiment and Result

In this section, an experiment is conducted using the proposed fully connected neural network. 16800 conductivity change vectors are used to train and validate the fully connected neural network, after the training, the model performance on 4200 testing samples using MSE gives the testing error of 1.08×10^{-3} , by comparing the predicted output and the annotation, the average difference between the predicted and true center position is 0.00591m. Fig.5.11. shows the training process of the neural network.

5.4 Conclusion

According to our experiments, the machine learning models especially neural networks can be built for the damage prediction given EIT generated conductivity change data. In this study, we use EIT images and conductivity change vectors as input separately to predict the number, radius and center position of damage holes, the comparison between the performance of models with different inputs is shown in the Table 5.6. and Fig.5.12.. From the comparison, we can clearly see that the conductivity change vector is a better option as input and the main reason may be that the process of constructing images from vectors causes the loss of details.

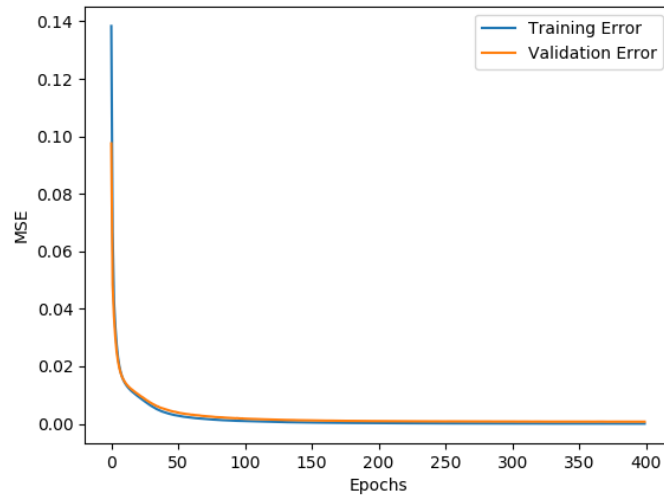


Fig. 5.11. Training process of the FCNN predicting the center position of holes

Table 5.6.

Comparison of performance between using EIT images and conductivity change vectors as input

Prediction Goal	Metrics	EIT Images	Conductivity Change Vectors
Hole number	Testing accuracy	0.892	0.995
Hole radius	Average difference between predicted and true radius (m)	0.00765	0.000872
Center position	Average distance between predicted and true center positions (m)	0.0172	0.00591

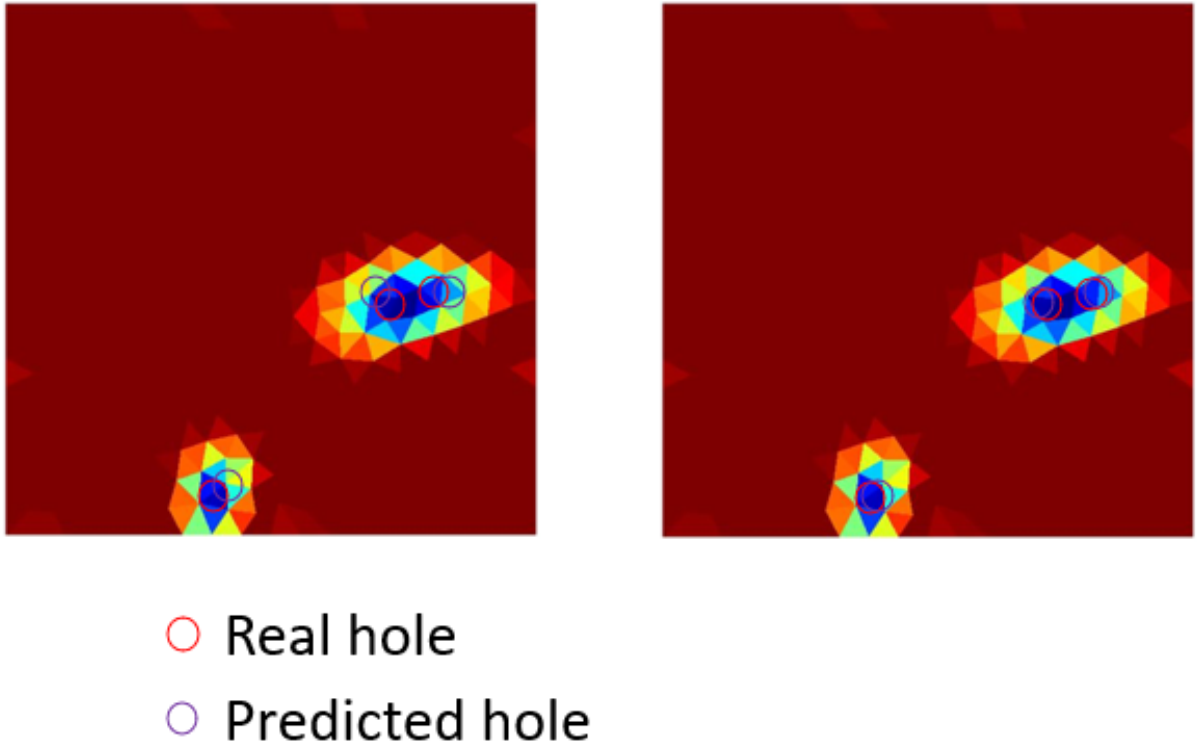


Fig. 5.12. Comparison of performance between using EIT images and conductivity change vectors as input

6. SUMMARY

Our study is a very first attempt of combining neural networks with EIT method to detect the damage on the self-sensing material and from our empirical results, our methods have a good performance. Compared to the traditional ways of using EIT for damage detection, our method not only detects the existence of damage but also gives a much more precise description of the damage status, including the number, center position and size of damage, and after our models are well trained, they can achieve the real-time and accurate damage detection for new samples, with these advantages, our study has a great potential to the field of structural health monitoring.

Of course, our study still has the space of improvement, first, the size of damage studied in our research is not very small compared to the size of specimen, so we need to improve our method for detecting smaller damage, second, the number of damage holes in our study is limited between 1 to 3, we need to increase the number of damage holes that our method can handle and third, the damage studied in our research is only circular holes, damage in different categories and shapes should be considered in our future work.

REFERENCES

REFERENCES

- [1] C. R. Farrar and K. Worden., *An Introduction to Structural Health Monitoring*. Philosophical Transactions. Series A, Mathematical, Physical, and Engineering Sciences, 365(1851), 2007.
- [2] K. Loh, J. Hou, T.-C. Lynch, and J. Kotov., *Carbon Nanotube Sensing Skins for Spatial Strain and Impact Damage Identification*. Journal of Nondestructive Evaluation, 28(1), 9-25, 2009.
- [3] H. Dai, G. Gallo, J. Schumacher, and T. Thostenson., *A Novel Methodology for Spatial Damage Detection and Imaging Using a Distributed Carbon Nanotube-Based Composite Sensor Combined with Electrical Impedance Tomography*. Journal of Nondestructive Evaluation, 35(2), 1-15., 2016.
- [4] S. Gupta, J. G. Gonzalez, K. J. Loh, and F. Kopsaftopoulos., *Self-sensing Concrete Enabled by Nano-engineered Cement-aggregate Interfaces*. Structural Health Monitoring, 16(3), 309-323., 2017.
- [5] T. Tallman, S. Gungor, G. Koo, and C. Bakis., *On the Inverse Determination of Displacements, Strains, and Stresses in a Carbon Nanofiber/polyurethane Nanocomposite from Conductivity Data Obtained via Electrical Impedance Tomography*. Journal of Intelligent Material Systems and Structures, 28(18), 2617-2629., 2017.
- [6] Y. Cha, W. Choi, G. Suh, S. Mahmoudkhani, and O. Büyüköztürk, *Autonomous Structural Visual Inspection Using Region-Based Deep Learning for Detecting Multiple Damage Types*. Computer-Aided Civil and Infrastructure Engineering, 33(9), 2018.
- [7] P. Ashwin, S. Coombes, and R. Nicks., *Mathematical Frameworks for Oscillatory Network Dynamics in Neuroscience*. The Journal of Mathematical Neuroscience, 6(1), 1-92., 2016.
- [8] S.-J. Lee, T. Chen, L. Yu, and C.-H. Lai., *Image Classification Based on the Boost Convolutional Neural Network*. IEEE Access 6 (2018): 12755-2768., 2018.
- [9] P. Chris, "K Means," <https://stanford.edu/~cpiech/cs221/handouts/kmeans.html>, 2012.